ANL-7373

Argonne National Laboratory

DETERMINATION OF GAMMA-RAY HEATING IN A CRITICAL FACILITY BY THERMOLUMINESCENT DOSIMETRY

by

George S. Stanford and Ted W. Johnson

DISCLAIMER

The facilities of Argonne National Laboratory are owned by the United States Government. Under the terms of a contract (W-31-109-Eng-38) between the U. S. Atomic Energy Commission, Argonne Universities Association and The University of Chicago, the University employs the staff and operates the Laboratory in accordance with policies and programs formulated, approved and reviewed by the Association.

MEMBERS OF ARGONNE UNIVERSITIES ASSOCIATION

The University of Arizona
Carnegie-Mellon University
Case Western Reserve University
The University of Chicago
University of Cincinnati
Illinois Institute of Technology
University of Illinois
Indiana University
Iowa State University
The University of Iowa
Kansas State University
The University of Kansas
Loyola University
Marquette University
Michigan State University
The University of Michigan
University of Minnesota
University of Missouri
Northwestern University
University of Notre Dame
The Ohio State University
Ohio University
The Pennsylvania State University
Purdue University
Saint Louis University
Southern Illinois University
University of Texas
Washington University
Wayne State University
The University of Wisconsin

Printed in the United States of America
Available from
Clearinghouse for Federal Scientific and Technical Information
National Bureau of Standards, U. S. Department of Commerce
Springfield, Virginia 22151
Price: Printed Copy $3.00; Microfiche $0.65

ANL-7373
Reactor Technology
(TID-4500)
AEC Research and
Development Report

ARGONNE NATIONAL LABORATORY
9700 South Cass Avenue
Argonne, Illinois 60439

DETERMINATION OF GAMMA-RAY HEATING IN A CRITICAL FACILITY BY THERMOLUMINESCENT DOSIMETRY

by

George S. Stanford and Ted W. Johnson

Reactor Physics Division

February 1968

THIS PAGE
WAS THIS PAGE ALLY
WAS INTENTIONALLY
LEFT BLANK

TABLE OF CONTENTS

TABLE OF CONTENTS

LIST OF FIGURES

LIST OF FIGURES

LIST OF TABLES

DETERMINATION OF GAMMA-RAY HEATING IN A CRITICAL FACILITY BY THERMOLUMINESCENT DOSIMETRY

by

George S. Stanford and Ted W. Johnson

ABSTRACT

Because of good sensitivity, small probe size, and relative ease of handling, thermoluminescent dosimetry (TLD) provides a useful method for measuring gamma-ray heating in critical facilities. The Bragg-Gray principle of cavity ionization is useful in analyzing the data if thin layers of phosphor, surrounded only by the material in which heating is to be measured, are used. Measurements made during critical experiments for the Argonne Advanced Research Reactor are reported. The phosphor used was CaF_2:Mn. Investigation of sensitivity to thermal and fast neutrons failed to reveal any appreciable perturbations under the experimental conditions encountered. Reproducibility of relative measurements was about 5-10%, which was adequate for the purpose; refinements in technique could improve on that. For absolute measurements, there were additional uncertainties: ±15% in the measurement of the absolute power of the critical facility, and approximately ±10% in a spectrum correction factor.

I. INTRODUCTION

In the design of a high-power reactor, knowledge of the gamma-ray heating is needed both for determining cooling requirements and for predicting where thermal stresses will be important. The work reported here was undertaken to facilitate the design of the Argonne Advanced Research Reactor (AARR), for which purpose measurements of gamma-ray heating in the preliminary critical assembly were desired.

Thermoluminescent dosimetry (TLD) was used to make the measurements. This is a less direct approach than calorimetry, but calorimetric measurement of gamma-ray heating rates in critical assemblies is very difficult, since the gamma flux at a typical power level of 50-100 W would cause a temperature rise of only about 10^{-3} °C/hr, assuming perfect insulation of the calorimeter. Consequently, the possibility of an indirect

measurement was considered, and it was concluded that an ionization detector would provide the desired information with the requisite sensitivity. TLD was selected, in preference to an ionization chamber, because of the inherently smaller probe size and the possibility of making simultaneous measurements at many different positions. A photographic emulsion was also considered, but it seemed that TLD was potentially more reproducible, easier to handle, and had a larger useful range. It has been reported that the CaF_2:Mn phosphor has a linear range of six decades or more.[1]

The methods reported here could be refined further. Work on this project was terminated, at least temporarily, along with termination of the critical experiments for the AARR. However, the desired experimental information was obtained from the TLD work, the accuracy requirements not being particularly stringent. This point is discussed later (Section V.B).

II. THEORY

A. Principle of Thermoluminescent Dosimetry

In brief, the principle of TLD is this: An ionizing particle, in passing through a suitable crystalline material, raises electrons into the conduction band, and some of these electrons, instead of falling directly back to the ground state, are captured in trapping centers at some intermediate energy level. The trapped electrons cannot get to a lower energy state except by first returning to the conduction band. In a material suitable for TLD work, the energy required to raise the trapped electrons back to the conduction band is not available from thermal motion at room temperature, but becomes available when the temperature is raised to approximately 200-300°C. In subsequently falling from the conduction band, the electrons emit visible-wavelength radiation, which can be detected by a photomultiplier tube. Further details are contained in Refs. 1 and 2.

The two most commonly used phosphors for TLD purposes are lithium fluoride and calcium fluoride, activated with a suitable material to provide the trapping centers. These powders can be irradiated and then stored for protracted periods before being read out. Readout can be accomplished with 5 mg or less of the powder, but normally a larger sample than this will be irradiated to permit two or more readings to be made. Calibration is accomplished by exposing samples from the same batch of powder in a known gamma-ray field.

B. Bragg-Gray Principle of Cavity Ionization

Interpretation of the measurements is based on the Bragg-Gray theory of cavity ionization,[3-7] with the recognition that there are some uncertainties in its application to TLD detectors, particularly for low-energy

electrons. The standard formulation of the Bragg-Gray principle is

$$D = P \cdot W \cdot J,$$

where D is the dose in the wall material, in ergs/g or rads; P is the mass stopping power for electrons in the wall, relative to the mass stopping power of the detecting material; W is the energy required to create an ion pair in the detector, and J is the number of ion pairs created per gram of detector. For this formula to hold, the following two conditions must be met: The wall must be thicker than the range of the primary electrons being detected, and the detecting material must be thin enough so that the electrons passing through it lose only a small part of their energy. Under these conditions, the response of the detector is a function of the rate of interaction of the gamma rays with the wall material, not with the detecting material. If the latter has, in effect, the same atomic number as the wall material, the requirement that the detecting material be thin can be relaxed.

The Bragg-Gray theory has been refined by Spencer and Attix,[7] who have tabulated values of a quantity $f_z(T_0, \Delta)$, defined to be the total energy dissipated per gram of air (in an air-filled ionization chamber), divided by the total energy dissipated per gram of wall material. Here z refers to the wall material, T_0 is the initial kinetic energy of the electrons, and Δ is the kinetic energy that an electron must have to traverse the cavity. The results of their calculations are shown in Table I, which gives the basis of the f_z values used in the course of this work. Interpolating or extrapolating was done where necessary.

TABLE I. Values for $f_z(T_0, \Delta)$, as Calculated by Spencer and Attix[7]

[Energies T_0 and Δ are in units of mc^2, and the stopping powers used were in units of $mc^2/(gm/cm^2)$]

Atomic Number	Element	T_0	Δ = 0.005	0.01	0.02	0.04	0.08	0.16
			$f_z(T_0, \Delta)$					
6	C	2.56	0.986	0.987	0.988	0.988	0.989	0.989
		1.28	0.985	0.986	0.987	0.988	0.988	0.989
		0.64	0.985	0.986	0.987	0.987	0.988	0.989
13	Al	2.56	1.161	1.149	1.140	1.133	1.126	1.122
		1.28	1.169	1.155	1.145	1.137	1.131	1.126
		0.64	1.175	1.161	1.151	1.143	1.136	1.130
29	Cu	2.56	1.444	1.400	1.369	1.347	1.329	1.315
		1.28	1.465	1.417	1.384	1.360	1.342	1.325
		0.64	1.485	1.435	1.400	1.375	1.354	1.337
50	Sn	2.56	1.784	1.691	1.631	1.589	1.557	1.532
		1.28	1.822	1.723	1.659	1.613	1.580	1.551
		0.64	1.861	1.756	1.687	1.640	1.602	1.571
82	Pb	2.56		2.053	1.939	1.864	1.809	1.769
		1.28		2.104	1.985	1.904	1.848	1.801
		0.64		2.161	2.030	1.946	1.882	1.832

In the present work, the powdered TLD phosphor (CaF_2, activated with manganese) was irradiated in a thin layer of about 20 mg, contained in a disk-shaped capsule of the desired wall material. Commercial thermoluminescent dosimeters are available, with the phosphor presealed in small tubes. Although easier to handle and read out, these were not used because the powder thickness, the wall thickness, and the wall material were not suitable for useful application of the Bragg-Gray principle.

C. TLD Calibration

TLD probes must be calibrated by reading out, at the same time, samples of the same batch of phosphor which have been given a known gamma exposure X^c (roentgens) in a calibrated irradiation facility. The dose in air corresponding to a one-roentgen exposure is 0.869 rads, and the dose D_z^c (in rads) in a piece of material z is given by

$$D_z^c = 0.869\, X^c Y_z^c, \tag{2.1}$$

where Y_z^c is the ratio of the mass energy-absorption coefficient of material z to that of air, for the energy of the gamma rays in the calibration facility. The superscript c refers to the calibration facility.

At approximately 1 MeV, corresponding to the gamma-ray energy in a Co^{60} irradiation facility, selected values of Y_z^c are as follows:[8,9]

Lucite	Be	Fe	Al
1.075	0.886	0.932	0.961

Let A_z^c be the observed response of the TLD phosphor, in arbitrary units, irradiated in a capsule of material z in the calibration facility; and let g^c be a factor such that $g^c A_z^c$ is the dose that an air filling in the capsule would have received. Then from the definition of f_z,

$$f_z = \frac{g^c A_z^c}{D_z^c}. \tag{2.2}$$

D. Dose Determination

Consider first an irradiation in the critical facility, of a TLD sample in a capsule of the same material as used in the calibration exposure. Assume that f_z is the same in both cases, even though the prevailing gamma spectra are different. Table I indicates that, for the lighter elements, this assumption is probably good to ±2% or so. As before, then,

$$f_z = \frac{g^r A_z^r}{D_z^r}, \tag{2.3}$$

where the superscript r refers to the reactor. Combining Eqs. 2.2 and 2.3, we get for the desired dose

$$D_z^r = \frac{g^r}{g^c} \cdot \frac{A_z^r}{A_z^c} \cdot D_z^c . \tag{2.4}$$

TLD phosphors are reported to have diminished sensitivity to densely ionizing particles.[10] Since the ion density in electron tracks becomes larger for slow electrons, the TLD response can be expected to be somewhat sensitive to the gamma-ray spectrum. Thus g^r will not in general be equal to g^c. Determination of g^r/g^c will be discussed in Sections II.F and V.E.

Now consider the case in which the phosphor irradiated in the reactor was in a capsule of material x differing from the material z used in the calibration exposure. Then, as in Eq. 2.3,

$$f_x = \frac{g^r A_x^r}{D_x^r}, \tag{2.5}$$

and combining this with Eq. 2.2 gives

$$D_x^r = \frac{g^r}{g^c} \cdot \frac{f_z}{f_x} \cdot \frac{A_x^r}{A_z^c} D_z^c . \tag{2.6}$$

The quantities f_x and f_z can be determined (or deduced) from Table I. An assumption here is that g^r is the same for all capsule materials--that is, that the electron spectrum in the wall is not a strong function of the wall material.

Once D_x^r has been determined for a particular location in the reactor, the dose rate that would prevail in any other material w can be deduced. As in the case of Eq. 2.1, we can write

$$D_x^r = 0.869\, X^r Y_x^r \tag{2.7}$$

and

$$D_w^r = 0.869\, X^r Y_w^r, \tag{2.8}$$

leading to

$$D_w^r = \frac{Y_w^r}{Y_x^r} D_x^r . \qquad (2.9)$$

In Eq. 2.9, the mass energy-absorption coefficient for air cancels out, the quantity Y_w^r/Y_x^r reducing to the ratio of the mass energy-absorption coefficients of the two materials w and x, for the gamma-ray spectrum prevailing at the point of observation. Some values of this ratio are given in Section II.E.

E. Mass Energy-absorption Coefficients

The mass energy-absorption coefficient μ_{en}/ρ is a function of the gamma-ray energy and of the material. For irradiations in the gamma calibration facility, Y_z^c can be determined from tables[8,9] given the gamma-ray energy (see Section II.C). For the reactor spectrum, however, accurate determination of μ_{en}/ρ depends on a detailed knowledge of the gamma spectrum--particularly the low-energy end. The gamma-ray spectrum in the AARR critical assembly was not measured, but the results of some calculations with the MAC code were available[11] and were used in estimating effective values for μ_{en}/ρ.

Table II gives the calculated gamma spectra for two positions in the AARR: 10 and 96 cm beyond the edge of the core. The first position is inside the beryllium reflector; the second is at the wall of the pressure vessel. Effective values of μ_{en}/ρ were determined from these spectra by calculating the flux-weighted averages, according to

$$\frac{\mu_{en}}{\rho} = \frac{\sum_j (\mu_{en}/\rho)_j \gamma_j}{\sum_j \gamma_j}, \qquad (2.10)$$

where γ_j is the total gamma-ray flux in the jth energy group, in MeV/cm²-sec, from Table II. Unfortunately, the MAC code provided no breakdown of the low-energy group, 0-1 MeV. This is unimportant for the more distant position, since not much of the flux is in this group, but it is important for the 10-cm position. Consequently, for the inner position, μ_{en}/ρ was calculated on the basis of three different assumptions: (a) The effective value of μ_{en}/ρ for the low-energy group was the value

TABLE II. Calculated Gamma Spectra, AARR[11]

Energy Group, MeV	Gamma Spectra, arbitrary units	
	10 cm from Core	96 cm from Core
0-1	12	0.22
1-2	11	5.8
2-3	9.8	18
3-5	5.1	29
5-7	1.8	19
7-9	1.9	27
>9	0.57	6.8

at 0.8 MeV; (b) the effective value was the same as the 0.15-MeV value; (c) the flux in each 200-keV subgroup of the 0-1-MeV range was the same. In the latter case, the 0-1-MeV region was divided into five equal energy groups, and Eq. 2.10 was applied, with values of μ_{en}/ρ taken at energies of 100, 300, 500, 700, and 900 keV.[8,9]

The results of these calculations of the mass energy-absorption coefficients for several substances are given in Table III. The values for the low-Z materials beryllium, aluminum, and Lucite are not particularly sensitive, even here, to the low-energy gamma spectrum. For elements of higher atomic number, however, μ_{en}/ρ rises rapidly as the gamma energy drops below approximately 300 keV, which accounts for the spread in the iron values in Table III.

TABLE III. Effective Values and Ratios of μ_{en}/ρ at Two Distances from the AARR Core

	10 cm from Core			
	Assumed Effective Energy of 0.1-MeV Group			
Material	0.8 MeV	0.15 MeV	Flat	96 cm from Core
		μ_{en}/ρ, cm^2/g		
Be	0.0211	0.0200	0.0207	0.0157
Al	0.0239	0.0241	0.0245	0.0200
Fe	0.0245	0.0397	0.0362	0.0233
Lucite	0.0256	0.0243	0.0251	0.0190
		Ratios		
Be/Al	0.883	0.830	0.845	0.785
Be/Fe	0.831	0.504	0.572	0.674
Be/Lucite	0.824	0.823	0.825	0.826
Al/Fe	0.976	0.607	0.677	0.858
Al/Lucite	0.934	0.992	0.976	1.053

At the position of the pressure-vessel wall, the gamma spectrum is considerably harder, and the effective mass energy-absorption coefficient is insensitive to the gamma-flux shape in the 0-1-MeV region.

Note that the beryllium/Lucite ratio is virtually independent of the gamma-ray spectrum. Thus when Eq. 2.9 is applied to determine gamma heating in the beryllium reflector, TLD measurements made with Lucite capsules should be somewhat more reliable than those made with capsules of iron (stainless steel) or aluminum.

The sensitivity of the effective μ_{en}/ρ of high-Z elements, here exemplified by iron, to the details of the low-energy end of the gamma spectrum indicates that it is desirable to base predictions of heating rates in a high-Z material on measurements made in that material.

F. Determination of g^r/g^c

The ratio g^r/g^c, which depends on the difference between the calibration and reactor gamma-ray spectra (see Section II.C), can be determined empirically by an experiment using an ionization chamber. Let the chamber and some TLD capsules have walls of material z, with thickness greater than the range of the primary electrons. The chamber is irradiated in the calibrated gamma facility, and the ion current I^c is observed in the known gamma field. The chamber is then transferred to the reactor, and the current I^r is observed while a TLD sample is being irradiated at the same place, at constant power, for a known time t^r. A TLD sample is also irradiated in the gamma facility, at the same exposure rate as used for the chamber, for a time t^c.

The gas in the ionization chamber is not necessarily air. Let D_a^c be the dose received in time t^c by the gas filling, in the calibration exposure, and let f_z' be the ratio of the dose in the gas filling to the dose in the wall, so that

$$D_a^c = f_z' D_z^c. \tag{2.11}$$

For a TLD capsule, we have, from Eq. 2.2,

$$D_z^c = \frac{g_c A_z^c}{f_z}. \tag{2.12}$$

Combining Eqs. 2.11 and 2.12 leads to

$$D_a^c = \frac{f_z'}{f_z} g^c A_z^c, \tag{2.13}$$

and we can write, by analogy, the same equation for the reactor run,

$$D_a^r = \frac{f_z'}{f_z} g^r A_z^r. \tag{2.14}$$

Since $D_a^r/E_a^c = I^r t^r / I^c t^c$, it follows from Eqs. 2.13 and 2.14 that

$$\frac{g^r}{g^c} = \frac{I^r t^r}{I^c t^c} \cdot \frac{A_z^c}{A_z^r}. \tag{2.15}$$

An assumption here has been that the ratio f'_z/f_z is the same for the gamma spectra of both the calibration facility and the reactor, an assumption that is probably reasonable for most counter gases.

We have also assumed that the phosphor has no neutron sensitivity. If it does, however, then that effect will be included in the value of g^r/g^c as calculated by Eq. 2.15, and thus the gamma dose rates as calculated from Eq. 2.4 or 2.6 will automatically be corrected for the effect of the reactor neutrons.

III. EXPERIMENTAL METHOD

A. Phosphor

The TLD phosphor selected for these measurements was manganese-activated CaF_2, as manufactured by Edgerton, Germeshausen & Grier, Inc. Another possible choice, LiF highly depleted in Li^6, could perhaps cause trouble through the energetic $Li^6(n,\alpha)t$ reaction. Actually this might not have been the case, since TLD phosphor is relatively insensitive to densely ionizing particles.[10] However, fast neutrons could have presented another problem with LiF (see Section IV.F). Two disadvantages of the CaF_2 over the LiF are that the smaller grain size (at least in the material available) makes the CaF_2 somewhat harder to distribute uniformly in the readout pan, and that for readout it must be heated to a somewhat higher temperature, with a consequently greater background from thermal radiation from the heater components.

B. Calibration

Each time TLD samples were irradiated in the reactor, a more or less simultaneous irradiation was performed in a calibrated gamma-ray facility. The standard facility used was usually a calibrated Co^{60} facility operated by the Biology Division, but for some experiments a radium facility of the Industrial Hygiene and Safety Division was used. The calibration samples were given doses comparable to those expected in the reactor run, and they were read out along with the samples from the reactor.

C. Capsules for Irradiation

During this work, we discovered that exposing the CaF_2 TLD phosphor to water vapor would result in a spurious thermoluminescence (see Section IV.D). To exclude moisture during irradiation, capsules of the type shown in Fig. 1 were constructed of Lucite, aluminum, and stainless steel. The O-ring seal was adopted after less elaborate containment failed to exclude the moisture.

Some 15-20 mg of phosphor would be placed in each capsule. The thickness of the layer of powder was approximately 0.3 mm, which is not very thin in the Bragg-Gray sense, since that corresponds to the range of an electron with about 200 keV of kinetic energy. Assignment of effective values for T_0 and Δ (see Table I) was rather arbitrary, and fortunately this is not critical. If we assume that $T_0 \approx 1$ MeV, both for the Co^{60} irradiation facility and for the reactor, then $\Delta \approx 0.2$.

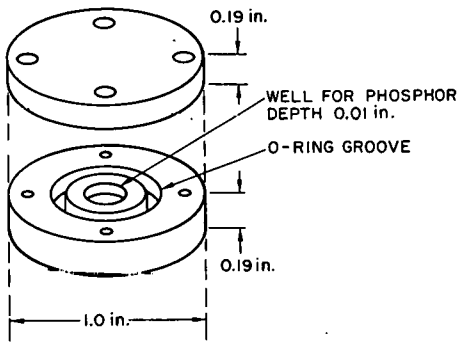

112-8370

Fig. 1. Capsule for Irradiating TLD Phosphor

D. Determination of f_z

On the basis of the above assignments, the values of f_z for some materials of interest were deduced from the data in Table I. The results are listed in Table IV, where the assigned errors come mainly from the uncertainty in interpolating and extrapolating from the data in Table I. The effective atomic number Z of Lucite was calculated from[12]

$$Z^3 = \frac{\sum_i a_i Z_i^4}{\sum_i a_i Z_i},$$

where a_i was taken to be the atom fraction of the element i.

TABLE IV. Values for f_z for $\Delta = 0.2$ and $T_0 = 1$ MeV

Material	f_z
Be	0.98 ± 0.03
C	0.990 ± 0.005
Lucite	1.01 ± 0.02
Al	1.13 ± 0.02
SS	1.29 ± 0.02
Cu	1.33 ± 0.03

E. Readout

The luminescence induced in the phosphor was determined by taking 2-5 mg of the irradiated powder and distributing it as evenly as possible in the bottom of a small silver pan, about 1/4 in. in diameter. The pan and powder were carefully weighed on a precision balance (Federal Pacific Model LG spiral-spring balance) with a reproducibility and a quoted accuracy of about ±0.025 mg. After being weighed, the pan and powder were placed in a readout apparatus, where heat was applied and the thermoluminescence was detected by a photomultiplier tube. At least two aliquots of each irradiation sample were read out, and the results were averaged. No systematic dependence on powder amount was observed in the light output per milligram, in the 2-6-mg range.

The main components of the readout equipment are indicated in Fig. 2. An EMI-6097S photomultiplier tube, which features fairly low dark current, was used. The S-type spectral response is compatible with the

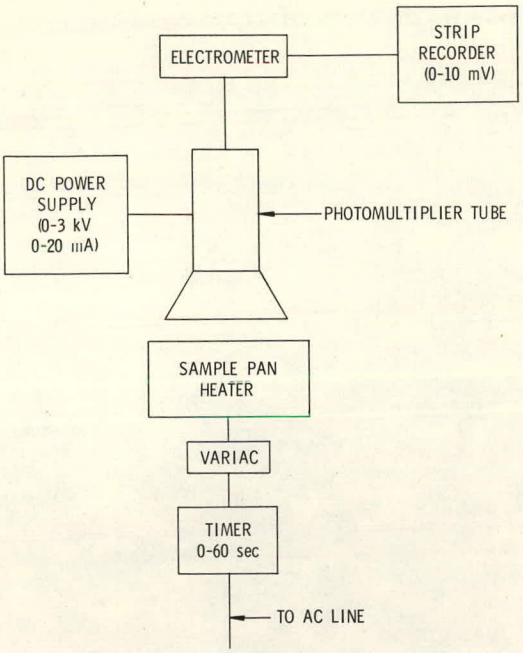

Fig. 2. Block Diagram of TLD Readout System

thermoluminescent emission spectrum of CaF_2:Mn.[7] (A phototube with very low dark current is needed only if rather small doses are to be measured; this was not a requirement here, since the doses ranged upward from approximately 5 rads. For more critical applications, the more expensive ASCOP-543D tube has sometimes been used.[13] Cooling the phototube should help to reduce the dark current. The signal can also be separated from the dark current by a chopping technique.[14])

The anode of the phototube was grounded through a 100 k resistor, shunted by a 2-μF capacitor for noise suppression. A Keithley Model 610BR electrometer was used to measure the voltage developed across the resistor, and the output was plotted on a strip-chart recorder. Figure 3 shows a typical chart record. The duration of heating was about 20 sec. The area under such curves was determined with a planimeter, although on a routine basis one would want to use a recorder with a built-in integrator. The height of the peak is regarded as a less reliable indicator of the dose than the area is, since the actual rate of heating of the powder in the pan is variable.

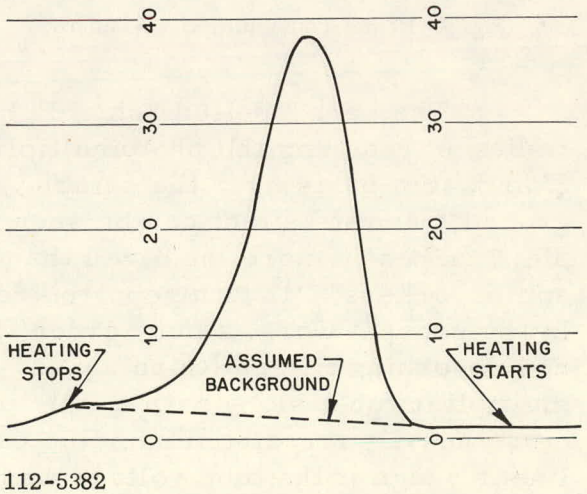

Fig. 3. Glow Curve for CaF_2:Mn TLD Phosphor. (Time scale goes from right to left.)

At least one day was allowed to elapse between irradiation and readout, since an initial rapid fading of a portion of the thermoluminescence has sometimes been reported,[1,15] although this apparently does not always happen.[1] No attempt to see such an effect was made in the course of this work.

Figure 4 is a photograph of the heater-photomultiplier assembly. A slightly modified soldering gun was used to pass current through a stainless steel heating element, on which the sample pan was placed. When the sample was to be changed, the shutter was closed to keep light from reaching the photomultiplier tube, and the upper assembly was lifted off, exposing

the parts seen in close-up in Fig. 5. The basic design of this system is due to Cameron et al.[16] and Kastner et al.[13]

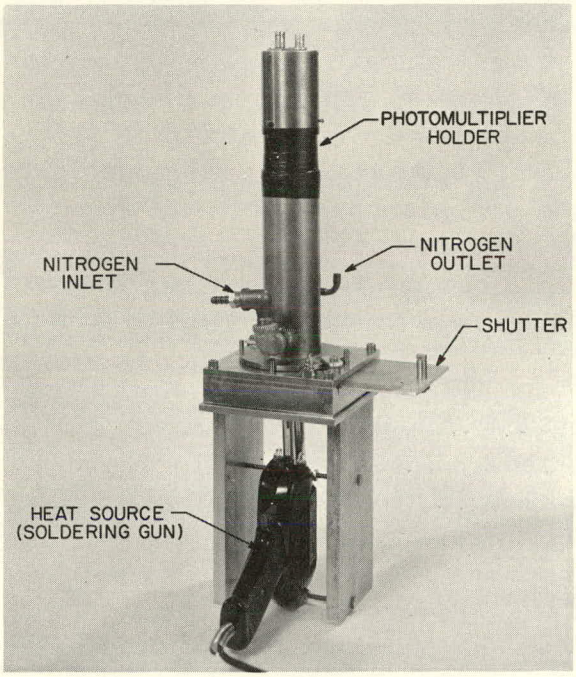

112-9600A

Fig. 4. Heater-Photomultiplier Assembly

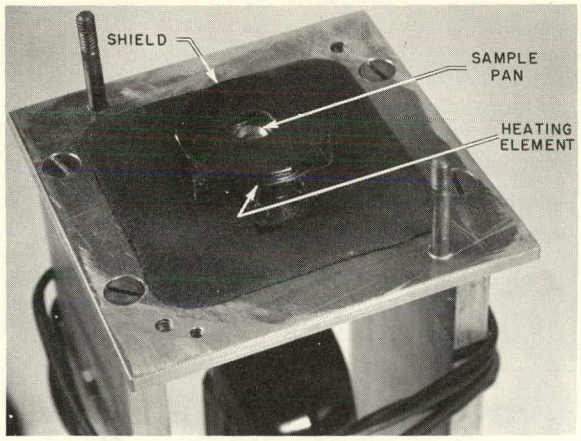

112-9601A

Fig. 5. Heater and Sample Pan

The part labelled "shield" helps reduce the amount of thermal radiation reaching the photomultiplier. This thermal radiation, coming from warm parts near the sample, is referred to as "black-body background," and its effect can be seen in Fig. 3. Radiant heating of the sample, inherently more localized than conductive heating, has been used by some workers,[15,17] with reported reduction in the black-body background. In the present work, a blue-green filter (Corning No. 4-76) and two infrared absorbing filters (Corning No. 1-69) were placed in front of the photomultiplier tube, along with a light pipe consisting of $1\frac{1}{2}$ in. of Lucite. The more heavily irradiated samples caused the tube current to exceed the linear range if the tube voltage was kept above the recommended minimum of 1150 V. An aluminum-foil diaphragm with a 1/2-in. hole was therefore put next to the face of the phototube. The components of the light path from the sample to the phototube were optically coupled with photomultiplier coupling grease (Dow-Corning No. C-2-0057).

IV. INVESTIGATION OF POSSIBLE PERTURBATIONS TO THE TLD MEASUREMENTS

A. General

Since the object of this work was to measure gamma-ray heating in the presence of neutrons, it was necessary to determine whether the results were being influenced by the neutrons. Capture of thermal neutrons by the phosphor components, and effects due to fast neutrons were considered and are discussed below. It was concluded on the basis of measurements and calculations that, for the conditions prevailing during these experiments, and within the precision of the measurements, no large neutron effect was discovered.

B. Water Vapor

A perturbing factor that did at first prove troublesome was water vapor. Exposing the CaF_2 powder to a humid atmosphere for a few hours resulted in a spurious reading equivalent to a dose of about 6 rads. Moreover, even with the powder stored in a desiccator and kept in darkness most of the time, a reading equivalent to a dose of a few rads would be accumulated over a period of time, and we concluded that the powder should be baked at about 400°C shortly before using it. Vacuum drying (at room temperature) failed to erase the effect of exposure to high humidity.

After less elaborate containment had failed to work, the O-ring seal shown in Fig. 1 was used to keep the powder dry while it was being irradiated (e.g., under water, in the reactor). Provided that there is a good O-ring seal, such a capsule seems to eliminate the water-vapor problem.

C. Neutron Capture by the Manganese in CaF_2:Mn

The CaF_2 TLD phosphor is activated by doping with a small percentage of manganese.[18,19] Capture of thermal neutrons by calcium or fluorine does not lead to production of heavily ionizing particles, and the cross sections for the emission of electrons are small, so that the manganese is the only component of the phosphor that needs to be considered in this connection. It has an appreciable cross section (13 barns) for thermal-neutron capture, and capture is followed by emission of a beta particle with energy ranging up to 2.9 MeV. However, most of the beta-particle energy is deposited in the wall of the capsule, rather than in the powder.

An experiment was performed to see whether the activation due to this process was appreciable.

First, the manganese content of the phosphor was determined by activation analysis. To make this measurement, some of the powder was

adulterated with a known amount of manganese tartrate ($MnC_4H_4O_6$), and both adulterated and unadulterated samples were irradiated simultaneously in a thermal-neutron flux. From the relative Mn^{56} activities, determined by gamma counting, it was calculated that the original phosphor was 2.0% manganese by weight.

A similar adulteration technique was used to investigate the thermoluminescent response to thermal-neutron capture by the manganese. Manganese tartrate was used because it is nonhygroscopic; it contains no isotopes other than Mn^{55} with an appreciable capture cross section for thermal neutrons; and it is white, thereby providing low interference with the readout efficiency.

Adulteration was accomplished by mixing for two minutes, in a vial vibrator, $MnC_4H_4O_6$ and CaF_2:Mn in the weight ratio of 1:9, thus somewhat more than doubling the manganese content. To check on the possibility that the mixing process, done with a small metal bead in the vial, might generate some thermoluminescence in the phosphor ("tribothermoluminescence"), some unadulterated phosphor was subjected to the same vibration process. Another possibility, that the presence of the adulterant somehow affects the observed light output, was checked by adulterating some phosphor after irradiation.

All the above types of samples, along with some straight $MnC_4H_4O_6$, were exposed to gamma rays in the radium irradiation facility. The relative responses were as given in Table V, which shows, at least within the experimental uncertainty of ±5%, that there is no evidence that the adulteration process itself leads to any spurious thermoluminescent response.

TABLE V. Relative Response of Various TLD Samples to 76 R of Radium Gamma Rays

Description of Sample	Relative Response per mg of CaF_2:Mn, ±5%
Adulterated before irradiation	1.14
Adulterated after irradiation	1.12
Unadulterated, but vibrated	1.20
Unadulterated, not vibrated	1.14
Pure $MnC_4H_4O_6$	<0.02
CaF_2:Mn, vibrated but not irradiated	<0.02

Two samples, one each of adulterated and unadulterated powder, were irradiated simultaneously at the inner tip of a radial beam tube in the AARR critical facility. Then a second such run was made with the positions of the adulterated and unadulterated samples interchanged. At that location

there was approximately 3 cm of beryllium between the samples and the core, making it a position where both the thermal- and fast-neutron fluxes were rather high. Averaging the results of the two runs yielded a ratio of 1.06 for the response of the adulterated sample to that of the unadulterated one, again with an estimated accuracy of ±5%. Thus, on the basis of this experiment, as much as 10% of the response of the unadulterated phosphor might have been due to neutron activation of the manganese. At the same time, since the manganese tartrate contained some hydrogen, some of the response of the adulterated sample might have been due to recoil protons.

Although this experiment leaves some questions unanswered, it showed that the quantitative importance to this work was marginal, and the matter was not pursued further. As was mentioned in Section II.F, emperical determination of the g^r/g^c ratio automatically introduces compensation for neutron sensitivity. As is noted in Section V.E below, the measurement of this ratio gives additional indication that any response to neutron capture by the manganese is not large.

D. Spurious Trap Creation

Certain dislocations in crystal lattices can act as electron traps, and such dislocations can be created by the recoil of a nucleus upon emission of a gamma ray following thermal-neutron capture, or upon an elastic interaction with an energetic neutron. To check on the formation of permanent traps by neutrons, an experiment was performed in which two lots of phosphor were given roughly the same dose, one in the reactor and the other in a neutron-free gamma field. The trapped electrons in both lots were released by heating. Both lots of powder were then reirradiated in a gamma facility. The measured thermoluminescent responses agreed to within 1%, which is well within the estimated experimental uncertainty of 3%. Thus there was no significant permanent change in the trap population due to neutron irradiation.

There was still the possibility that traps could have been created which were destroyed by the subsequent heating. Section IV.E below describes an experiment that bears on this.

E. Trap Emptying by Fast Neutrons

A "neutron-erasing effect" has been reported for LiF TLD phosphor.[20] Fast neutrons seemed to have the effect of removing electrons from their traps, thereby erasing some of the stored information. Consequently an experiment was performed to see whether, under the conditions prevailing in this work, such a phenomenon was observable in CaF_2 phosphor.

Three irradiations were performed, using six samples of phosphor in the combinations indicated in Table VI. The two irradiations in the Co^{60} facility were for 500 R each, and the dose received by the samples in the reactor was about 800 R. The samples in the reactor were separated from the core by about 10 cm of beryllium; thus the fast-neutron flux was not as great as it would have been closer to the core, but the conditions corresponded to those of most of the other measurements.

TABLE VI. Irradiation Sequence and Probe Response in Experiment to Investigate Neutron Erasing

TLD Sample No.	A	B	C	D	E	F
Irradiation						
First: Co^{60}	x	x				x
Second: Reactor		x	x		x	
Third: Co^{60}			x	x		x
Relative response, ±3%	0.920	2.373	2.436	0.952	1.516	1.834
Symbol	A^c	A^{cr}	A^{nd}	A^d	A^n	A^{cd}

All the irradiations were made on the same day. After the usual wait of about two days, the samples were read out, with results as listed in Table VI. The different responses will be referred to by the symbols given in that table. Also, let q be the fraction of the initial response A^c erased by the reactor neutrons. Then the total response A^{cr} of sample B is given by

$$A^{cr} = (1 - q) A^c + A^r, \tag{4.1}$$

which can be solved for q to yield

$$q = \frac{A^r - A^{cr} + A^c}{A^c}. \tag{4.2}$$

We can also write

$$A^{rd} = A^r + A^d. \tag{4.3}$$

Now A^r can be eliminated from Eqs. 4.1 and 4.3 to give an alternative expression for q,

$$q = \frac{A^{rd} + A^c - A^{cr} - A^d}{A^c}. \tag{4.4}$$

Inserting the responses from Table VI into Eqs. 4.2 and 4.4, and assuming an experimental uncertainty of 3% in each number, we get two partially independent values for q; they are, respectively, 0.068 ± 0.096, and 0.034 ± 0.118. Thus it can be said that there was no significant indication of a neutron-erasing effect under the conditions of this experiment.

(The datum for Sample F was not used in the above analysis. However, it provides a check on the consistency of the measurements, in that we should have $A^c + A^d = A^{cd}$, and this is in fact the case to within 2%.)

An alternative approach to the above data is to assume that there is no neutron-erasing effect, and to look for evidence of trap creation by the reactor neutrons. Let t represent the fractional increase in the number of traps, due to the reactor irradiation. Then

$$A^{rd} = A^r + (1+t)\, A^d, \tag{4.5}$$

from which

$$t = \frac{A^{rd} - A^r - A^d}{A^d}. \tag{4.6}$$

Combining this with $A^{cr} = A^c + A^r$ leads to the alternative expression for t,

$$t = \frac{A^{rd} + A^c - A^{cr} - A^d}{A^d}. \tag{4.7}$$

The resulting two values of t are, then, -0.034 ± 0.096, and $+0.033 \pm 0.118$. Here again, there is no evidence of spurious trap creation.

F. Dose due to Neutron Slowing Down

In a fast-neutron flux, energy will be imparted to the TLD phosphor by recoil nuclei, particularly, in the case of CaF_2, fluorine nuclei. Probably some thermoluminescence will be induced, although possibly not commensurate with the energy involved, in view of the previously mentioned reduced sensitivity to densely ionizing particles.[10] The predicted rate of energy deposition in the phosphor, due to this cause, was calculated for the reflector of the AARR.

The absorbed dose rate D(E) due to elastic recoil from neutrons of energy E is given by[4]

$$D(E) = E\phi(E) \cdot U, \tag{4.8}$$

where

$$U = \sum_i n_i \sigma_i \frac{2A_i}{(1+A_i)^2},$$

and

$\phi(E)$ is the differential neutron flux at energy E;

n_i is the number of atoms of type i per gram of material;

σ_i is scattering cross section, assumed here to be independent of E;

A_i is the atomic weight of element i.

For CaF_2, $U = 5.50 \times 10^{-3}$ cm^2/g.

To determine the total dose rate due to neutrons of all energies, Eq. 4.8 must be integrated over the neutron spectrum. For this purpose we used a 16-group spectrum calculated by the REX code for a position in the AARR beryllium reflector 2.0 cm from the edge of the core.[21] The effective mean energy for each of the six groups above 17 keV was determined by weighting according to a fission-neutron spectrum.

The calculations indicate that a CaF_2 sample 2.0 cm from the AARR core would absorb energy due to neutron slowing-down at a rate of 2.25 rad/min, at a reactor power of 50 W. The dose rate observed at this position in a TLD measurement was 110 rad/min. Thus not more than 2% of the observed thermoluminescent response should be due to recoil nuclei, and probably considerably less, because of the ion-density dependence. Moreover, the situation improves as we proceed outward from the core, since the fast-neutron flux falls off more rapidly than the gamma flux.

For LiF, $U = 21.9 \times 10^{-3}$, which is about four times the U for CaF_2. Thus, although the neutron slowing down could be ignored for CaF_2, this might not have been the case for LiF phosphor.

G. The $F^{19}(n,\alpha)$ Reaction

The reaction $F^{19}(n,\alpha)\ N^{16}$ occurs with a cross section rising approximately linearly from zero at a neutron energy of 3 MeV to 0.3 barn at 6 MeV, and with a Q-value of -1.49 MeV. The N^{16} decays with a 7.3-sec half-life to O^{16}, with a total decay energy of 10.4 MeV, of which an average of 5.7 MeV is in beta particles and neutrinos, and the rest is in gamma rays.

An accurate calculation of the energy imparted to CaF_2 TLD phosphor by this mechanism would be difficult, but an upper-limit calculation

is not. For this latter calculation, the following assumptions will be made, all of which are realistic or conservative: (a) all the alpha-particle energy is dissipated in the phosphor; (b) half the 5.7-MeV beta-decay energy is carried off by neutrinos; (c) half the remaining beta-particle energy is dissipated in the phosphor; (d) none of the gamma-ray energy is taken up by the phosphor; and (e) no prompt gammas accompany the (n,α) reaction--that is, all the available energy is imparted to the alpha particle.

The $F^{19}(n,\alpha)$ reaction occurs only for energies in the highest-energy REX group (see Section F above), which has a lower limit of 3 MeV. Conservatively, we will assume that the entire flux in this group occurs at 6 MeV, where the (n,α) cross section is 0.3 b. At a reactor power of 50 W, and at the previously mentioned position 2 cm from the core, the flux ϕ in this highest-energy group is calculated to be 2.4×10^7 n/cm^2-sec.

On the basis of the above considerations, the upper limit D to the total dose rate due to the $F^{19}(n,\alpha)\ N^{16}(\beta^-)\ O^{16}$ reaction is given by

$$D = n\sigma\phi(E_n - E_Q + 5.7/4), \qquad (4.9)$$

where

n is the number of F^{19} atoms per gram of phosphor;

σ is the $F^{19}(n,\alpha)$ cross section, 0.3 b;

E_n is the incident neutron energy, 6 MeV;

E_Q is 1.49 MeV, the magnitude of the (negative) Q value;

and

$5.7/4$ is the assumed energy left in the phosphor by the beta particles, in MeV per particle.

The result of this calculation is that, at the power and location mentioned above, the upper-limit dose rate from this reaction is 0.63 rad/min, which is less than 0.6% of the observed gamma dose rate (see Section F above) and therefore is negligible.

V. GAMMA-HEATING MEASUREMENTS IN THE AARR CRITICAL FACILITY

A. The Reactor

The Argonne Advanced Research Reactor (AARR) will operate at 100 MWt or more, to provide researchers with a high neutron flux.[22] To assist in the design, a series of critical experiments was performed, during which this TLD work was done. The core of the critical assembly had a hexagonal geometry, with a central light-water thermal column 6 or 7 cm in radius surrounded by an annular fuel zone approximately 17 cm thick. (See Fig. 6 below.) Highly enriched uranium was used, and the fuel zone had a metal/water volume ratio close to unity, causing the neutron spectrum in the core to be undermoderated. Surrounding the fuel region was a reflector consisting of about 30 cm of beryllium. The assembly was located at the center of a 3-m-diam tank, which could be filled with water to achieve criticality. A fuller description of the critical facility has been published elsewhere.[23] The TLD irradiations were typically made in runs of 15-30-min duration, at powers in the 20-300-W range.

Several cores, with differing amounts of fuel, were assembled in the critical facility. The excess reactivity of the heavier loadings was cancelled by incorporating into the loading boron-poisoned stainless steel strips. Table VII indicates the composition of the cores for the assemblies in which TLD measurements were made. Core 5 had a "graded" loading, in the sense that fuel plates near the inner and outer boundaries of the fuel region were thinner than the others, to reduce the power peaking in regions of high thermal-neutron flux. This assembly also had an internal thermal column (ITC) that was somewhat larger than for Cores 1-4a.

TABLE VII. Composition of AARR Critical Assemblies

Core No.	U^{235} Loading, kg	No. of Fuel Plates	No. of Boron-poisoned Strips	ITC Radius, cm
1	16.1	315	0	5.9
3	41.4	810	810	5.9
4a	62.1	1215	1620	5.9
5	57.3	1173	1089	7.2

The AARR will have a stainless steel pressure vessel with a 2.4-m (48-in.) radius, which will be penetrated by a number of beam tubes extending into or through the beryllium reflector. Predictions of gamma heating in the walls of the beam tubes, and in the pressure vessel near the penetrations, were desired, and the needed measurements were made in the critical facility. The results of these and other measurements are reported below.

Most of the TLD measurements were made with the graded, fully loaded core (Core 5)--the final one in the critical-experiment series. Where a measurement was made in one of the earlier loadings, this will be so stated.

B. Accuracy of the Measurements

The objective of this work was to measure absolute and relative gamma-ray heating rates at various locations near the core of the AARR critical facility. For the absolute measurements, it was necessary to make absolute power determinations in conjunction with the gamma-heating measurements. The power was determined from absolute counting of fission foils that were irradiated in a few selected locations in the core while the TLD run was being made. Given these local fission rates, it was necessary to do a numerical integration over the volume of the core. Because of various complexities, the most important probably being the presence of inserted control blades with resulting local flux depressions, the power was not determined with an accuracy better than ±15%.

A further consideration was that there were considerable differences in the detailed design of the critical facility and the projected research reactor, so that high-precision measurements in the critical facility would not in any event apply to the design reactor with equal precision. Absolute gamma-heating rates accurate in most cases to within 20% were obtained, and this was considered satisfactory. Relative heating rates, as in traverses along beam tubes, were not affected, either by the power uncertainties or by calibration errors and were obtained for the most part with a precision of ±5-10%. This, too, was adequate.

In view of these factors and the pressure of other work, no intensive effort was made to optimize the technique. The desired information has been obtained. Refinements can be introduced as the need arises.

C. Reactor Startup Source

The initial supply of neutrons needed to ensure safe startup of the AARR critical facility was provided by an activated sphere of antimony, about 15 mm in diameter, which was inserted into the beryllium reflector for the start of each run. (The neutrons are produced by the $Be^{9}(\gamma,n)$ reaction.) Sb^{124} has a 60-day half life. For most of the TLD measurements, the source was a fairly weak one, with negligible effect on the TLD samples at the total dose rates used. However, for some of the measurements a source that was more active by an order of magnitude was in place, necessitating a correction to the observed response of TLD samples that were not close to the core. The correction was determined by irradiating TLD samples under typical startup conditions, but without withdrawing control blades.

D. Time Corrections for Startup and Scram

The effective running time for each irradiation in the reactor was taken to be the time at power plus the period (the *e*-folding time, typically 40-60 sec) of the approach to power. In addition, for the TLD samples a correction was added to account for the post-scram gamma rays. The correction used was 33 sec, as determined by plotting the output of an ion-current chamber with a strip-chart recorder and determining the area under the decaying curve.

E. Measurement of g^r/g^c

The spectrum correction factor g^r/g^c was measured by the method of Section II.F, using stainless steel capsules and a specially built ion-current chamber with a stainless steel wall 3 mm thick, filled with argon at atmospheric pressure. For the reactor run, the chamber was located in a voided 4 x 4-in. radial beam tube, near the inner end. Between the tip of the beam tube and the core there was 10 cm of beryllium.

Two separate determinations yielded values of 1.28 and 1.12. Consequently the value used was 1.20, with an assigned uncertainty of ±10%.

In view of the diminished sensitivity of TLD phosphors to densely ionizing particles, a value of g^r/g^c greater than unity indicates that the gamma spectrum in the critical assembly, at least at the point where the measurement was made, has an appreciable low-energy component as compared with the Co^{60} spectrum (which consists predominantly of two lines, at 1.17 and 1.22 MeV). This agrees qualitatively with the calculational results in Table II for the 10-cm position.

Note also that any positive response to the reactor neutrons--e.g., capture in the manganese activant (see Section IV.C)--either is negligible or is more than cancelled by the spectrum effect. An appreciable negative response to neutrons was ruled out by the experiments described in Sections IV.E and IV.F.

Because of lack of time, the spectrum-correction factor was only measured at the one location, and all TLD measurements in the reactor were corrected by the observed value of 1.20. This is not strictly proper, as one would expect the correction to become smaller with increasing distance from the core, since (as indicated by the calculations) the gamma spectrum becomes harder. However, the magnitude of the change is not known, and moreover the uncertainty in this factor does not contribute greatly to the overall experimental error.

F. Traverses through the Beryllium Reflector

In the first and third loadings of the critical facility, measurements were made of the rate of decrease of gamma flux through a beryllium reflector that did not contain any beam tubes. The samples were located near the midplane of the reactor, in the positions indicated in Figs. 6 and 7. Figures 8 and 9 give the results. Because the power was not measured for the run of Fig. 8, and because of calibration inconsistencies affecting the data of Fig. 9, the ordinate scales give the observed dose in arbitrary units.

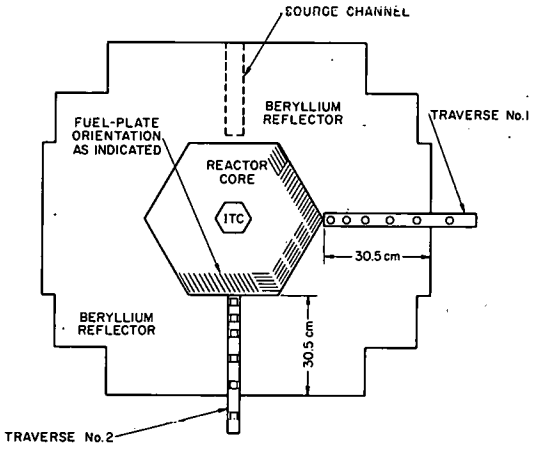

Fig. 6. Placement of TLD Samples in Reflector of Assembly No. 1

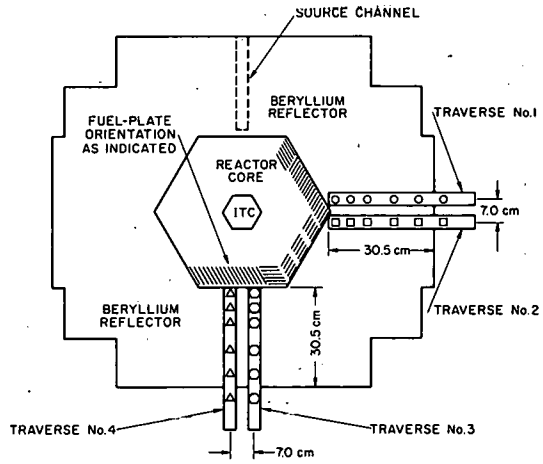

Fig. 7. Placement of TLD Samples in Reflector of Assembly No. 3

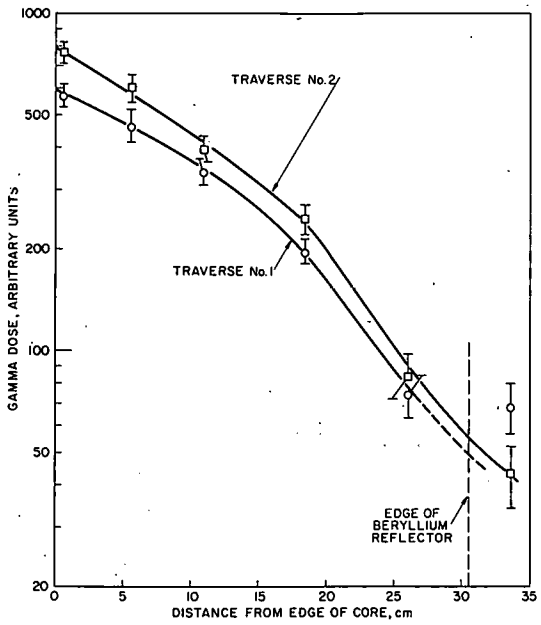

Fig. 8. Gamma Dose in Beryllium Reflector of Assembly No. 1. Probe locations are shown in Fig. 6.

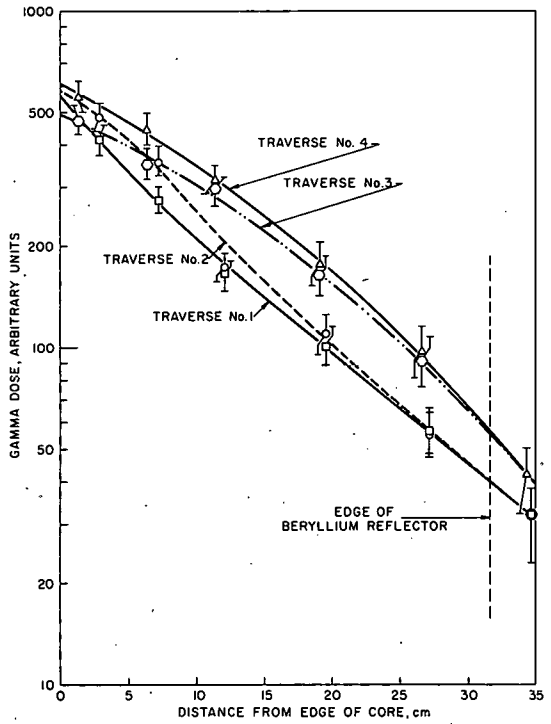

Fig. 9. Gamma Dose in Beryllium Reflector of Assembly No. 3. Probe locations are shown in Fig. 7.

These two experiments were done before the water-vapor problem (Section IV.B) was fully appreciated, and the phosphor samples were irradiated in shallow holes in Teflon strips, covered by waterproof Mylar tape. However, the doses were high enough so that the overall effect on the curves would not be large, although the points at the outer end might be high by about 10% (~6 rads). All control blades near the TLD samples were fully out of the core during the runs.

The abscissa of Figs. 8 and 9 is the distance from the TLD sample to the edge of the nearest fuel. Thus for Traverses 1 and 2 of Fig. 9, the distance is not measured along the line of traverse.

The relative amplitude of the two curves in Fig. 8 can be understood upon referring to Fig. 6, where it can be seen that two factors tend to give a higher dose rate to the samples for Curve 2 than for Curve 1. In the first place, Traverse 1 originates at a corner of the hexagonal core, whereas Traverse 2 starts at the center of one of the faces. Secondly, the orientation of the fuel plates in the core is relevant. Since uranium and stainless steel are both better absorbers of gamma radiation than water is, one would expect the gamma flux to be higher in a direction parallel to the surfaces of the plates than perpendicular to them.

The outermost point for Traverse 1 is anomalously high and is assumed to be a bad datum point.

Figure 9 shows that, for positions near the core, the points for Traverses 1 and 4 are higher, respectively, than for Traverses 2 and 3. For Traverses 1 and 2, it is reasonable to ascribe at least some of the difference to the effect of fuel-plate orientation. This is not so clear for the other pair of traverses (see Fig. 7), but it might be that lower gamma flux in the beryllium near the right-hand side of Traverse 3 influences the results of that traverse. At any rate, the differences seem to be real, since the reading-out was done in such a sequence as to prevent systematic differences, due to possible calibration drift, between the traverses in a pair.

The observed difference between Traverses 3 and 4 will be corroborated in Section G below.

The two lower curves in Fig. 9 differ in shape from the two upper ones. This is possibly accounted for by geometry differences, since Traverses 3 and 4 approach a corner of the hexagonal core, whereas the other two approach a flat face. We do not understand the shape differences between the curves for the first loading (Fig. 8) and those for the third (Fig. 9), since one would expect similar shapes even for the different fuel arrangements. However, the TLD technique was in the early development stage when the data for Fig. 8 were taken, and we cannot rule out the possibility that a repeat measurement would now yield different results.

G. Traverses in a Through Tube

In one of the experiments with the fully loaded, ungraded core (Assembly 4a), a 4-in.-square beam tube was installed, touching one of the core faces and passing completely through the beryllium reflector, as shown in Fig. 10.

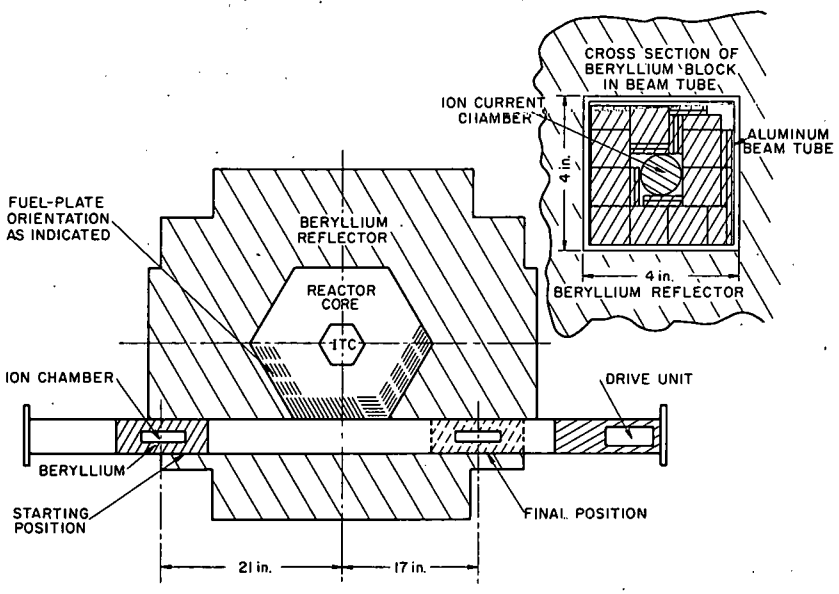

Fig. 10. Arrangement for Ion-chamber Traverse in Through Tube

An ion chamber, in a tube 1 in. in diameter and 6 in. long, was rather loosely packed in beryllium blocks, to make a package roughly $3\frac{5}{8}$ in. square and 12 in. long. The sensitive volume of the ion chamber was 0.7 in. in diameter and about 1 in. long. With the reactor running at constant power, this package was traversed along the otherwise voided beam tube by a motor drive unit, and the ion current was recorded as a function of the position of the chamber.

Then a second reactor run was made, this time with the portion of the beam tube inside the beryllium reflector filled with beryllium blocks surrounding a set of 23 TLD samples contained in a Teflon strip 3 mm thick by 24 mm wide.

Figure 11 shows the results of these traverses. The ion chamber gave a curve that is nearly symmetrical, whereas the TLD traverse did not. The latter, which was made in a beryllium-filled beam tube, again correlates with the fuel-plate orientation. It is not entirely clear why the asymmetry should not appear to the same extent in the ion-chamber traverse. However, observing that the beam tube was largely voided for the ion-chamber run, with only a relatively small amount of beryllium around the chamber, one can postulate that the effect is washed out because the ion chamber was responding to gamma rays originating in,

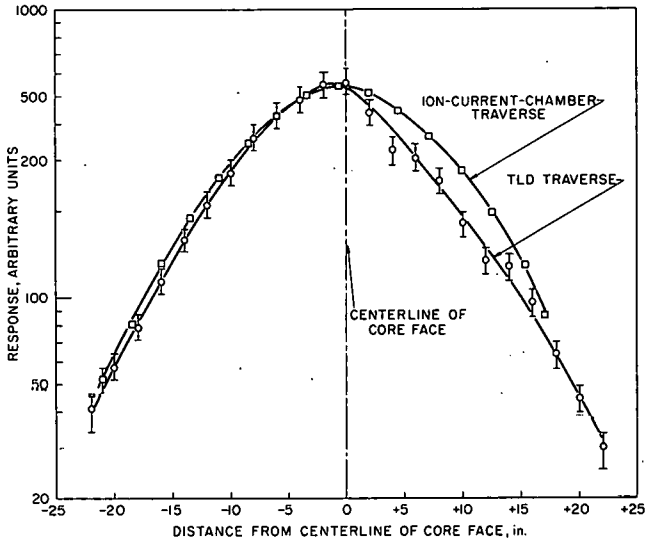

Fig. 11. TLD and Ion-chamber Traverses in Through Tube

or scattered from, a very much larger region than was the case for each TLD sample, which was small and closely surrounded by Lucite and beryllium.

The difference between the inner ends of Traverses 3 and 4 of Fig. 9 agrees well with the difference that would be predicted for on the basis of the TLD curve of Fig. 11, for a 7-cm separation.

H. Vertical Traverses in the Internal Thermal Column

A pair of vertical TLD traverses was performed in the internal thermal column (ITC) of Assembly 4a, with the samples located as shown in Fig. 12, contained in shallow holes in Lucite strips, covered by Mylar tape. The results are plotted in Fig. 13. For comparison, Fig. 13 also shows the results of a neutron activation traverse (U^{235} fissions) in the same assembly, arbitrarily normalized to the central TLD traverse at the midplane. As would be expected, the gamma dose falls off more slowly than the neutron flux outside the core.

The tendency to asymmetry in the TLD traverses is perhaps due to the presence of a partially inserted internal control blade during the run. (For the neutron-activation measurement, all internal control blades were withdrawn, control being by means of a peripheral blade.)

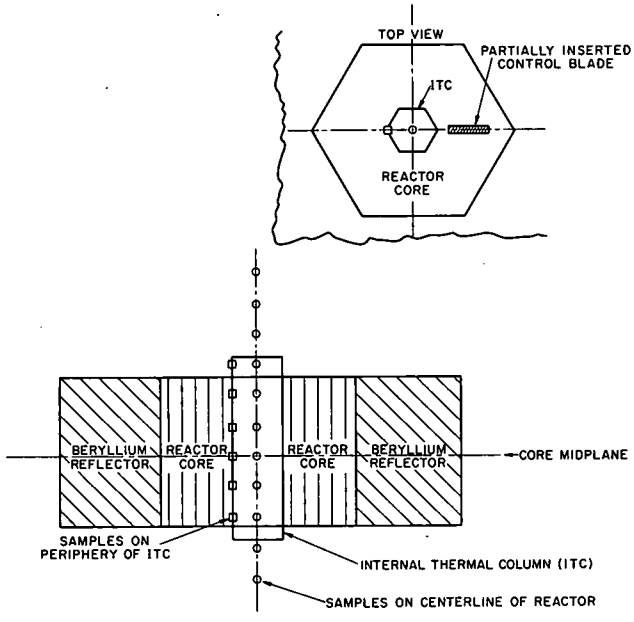

Fig. 12. Sample Placement for Vertical Gamma-heating Traverses in the Internal Thermal Column of Assembly No. 4a

The reactor power was not measured during the TLD run, and power calibration had to be based on the reactor instrument readings. Consequently, in addition to the experimental errors indicated in Fig. 13, there is an uncertainty of perhaps ±25% in the magnitude of the ordinate.

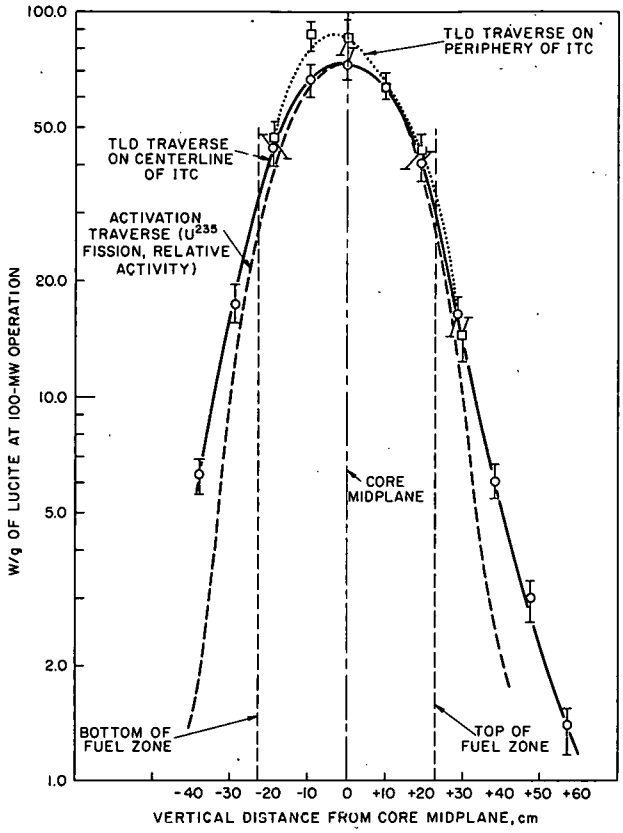

Fig. 13. Vertical Gamma-heating Traverses in the ITC of Assembly No. 4a. Probe locations are shown in Fig. 12.

I. Gamma Heating in Beam-tube Walls

The remaining TLD measurements, except one, described in this report were made in the AARR Critical Assembly No. 5, using the O-ring capsules shown in Fig. 1. Also, all the reactor runs for the following experiments were made with a control-blade configuration like the one expected for the power reactor. The six peripheral blades were banked with their tips about 2.5 cm below the top of the fuel, and the six internal blades were banked at whatever position was needed for criticality; this usually meant that they were about halfway in.

Figure 14 shows the sample locations for measurements of gamma heating in radial and tangential beam tubes. Several reactor runs were made, with voided aluminum-walled beam tubes, both 4 and 6 in. square, and with about 4 in. of beryllium between the tip of the beam tube and the core of the reactor. The TLD samples were in aluminum capsules, inside the beam tubes. In the radial tubes, the capsules were positioned along the centerline of the lower surface, and in the tangential tubes they were at the lower outside corner. The results of the different reactor runs were normalized by means of simultaneous power measurements, by TLD samples at standard monitor positions, or both.

The results for the radial tubes are shown in Fig. 15. The innermost points for the two tube sizes coincide, within experimental error, and from there the gamma flux falls off more rapidly in the 4-in. tube than in the 6-in. tube.

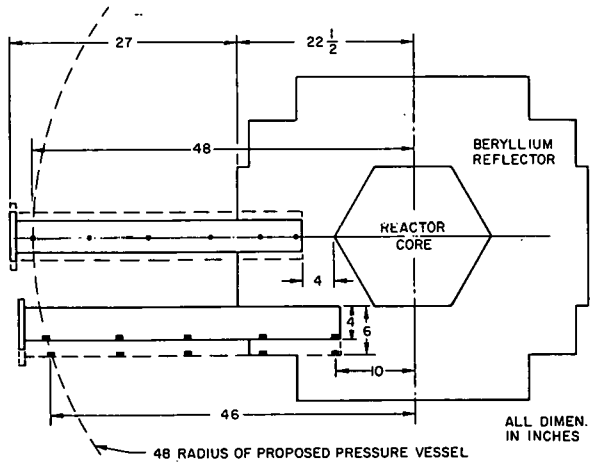

112-8371

Fig. 14. Sample Placement for Beam-tube Traverses, Assembly No. 5. Positions of both 4- and 6-in. beam tubes are indicated.

For the tangential tubes, the results are given in Fig. 16. Here the innermost points do not coincide, which is reasonable since the samples in the 6-in. tube were 2 in. farther from the reactor core. The error bars shown indicate the reproducibility of the measurements. Uncertainties in the power calibration lead to an additional systematic error of about ±15%.

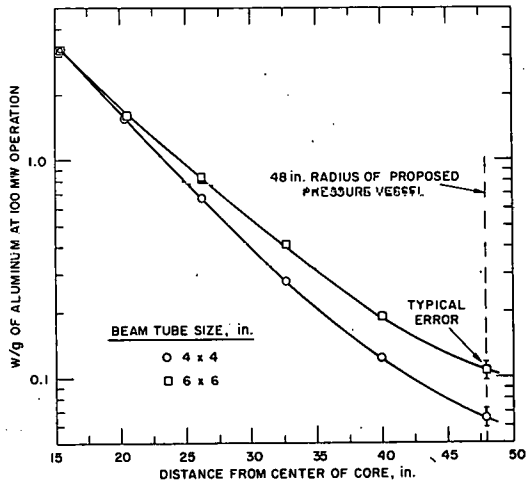

112-8365

Fig. 15. Gamma-heating Rates in Walls of Voided Radial Beam Tubes, with 4 in. of Beryllium between Core and Tip of Tube. Probe locations are shown in Fig. 14.

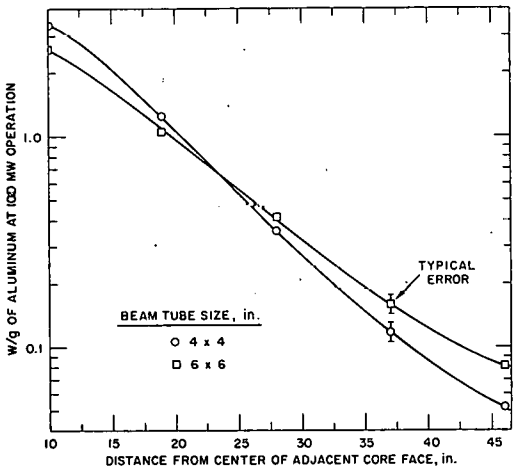

112-8369 Rev. 1

Fig. 16. Gamma-heating Rates in Walls of Voided Tangential Beam Tubes. Probe locations are shown in Fig. 14.

Some traverses similar to those of Fig. 15 were made in the radial beam tube, but with the tip of the beam tube touching the corner of the core. The results are given in Fig. 17, which indicates that when there is little or no beryllium between the tube and the core, the gamma dose rate is appreciably less at the tip of the 6-in. voided beam tube than for the smaller tube. The difference is ascribed to a local reduction in the fission rate in nearby portions of the core due to the void in the reflector, and this is consistent with an observed reactivity reduction caused by such voiding.

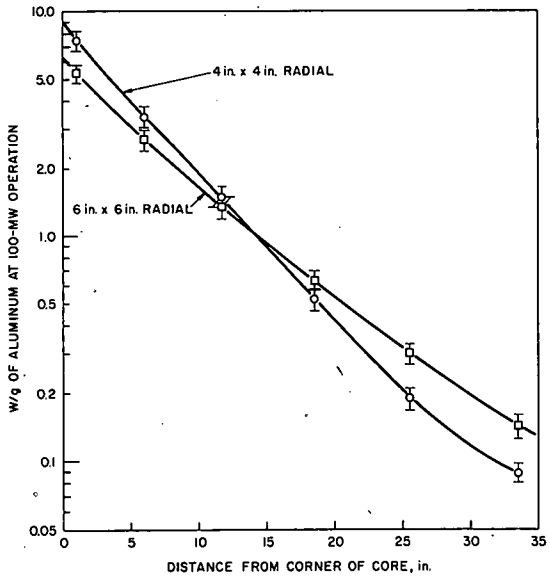

Fig. 17. Gamma-heating Rates in Walls of Voided Radial Beam Tubes, with Tip of Tube Touching Corner of Core

J. Gamma Heating at the Planned Location of the Pressure-vessel Wall

Some measurements were made to assist in predicting the gamma-ray heating to be encountered in the

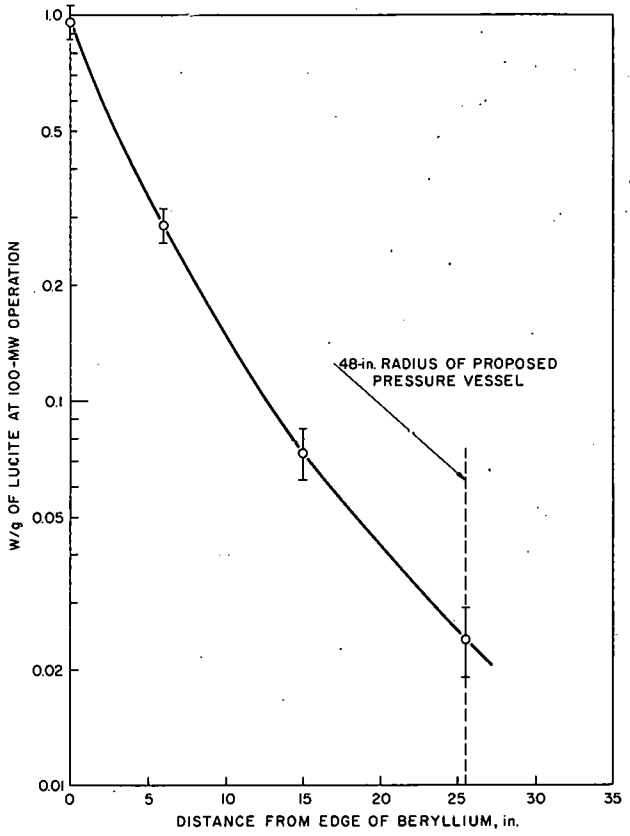

Fig. 18. Radial Gamma-heating Traverse in Water outside the Beryllium Reflector; Assembly No. 5.

stainless steel wall of the pressure vessel of the power reactor. The pressure vessel is to have a 48-in. radius.

Figure 18 shows the falloff in gamma heating in the water between the outer edge of the beryllium reflector and the pressure-vessel location, at the midplane. This traverse was made with Lucite capsules, at the side of the reactor 180° from the location of the radial beam tube (see Fig. 14); thus there were no beam tubes between the traverse and the core.

Thermal stresses due to gamma heating will be encountered in the wall of the pressure vessel, at the places where beam tubes penetrate it, due to gamma-ray streaming along the tubes. To help determine the magnitude of this effect, horizontal and vertical traverses were made (as shown in Fig. 19) extending from the walls of a tangential beam tube, with all samples 48 in. from the reactor centerline. The results are shown in Fig. 20, where it can be seen that,

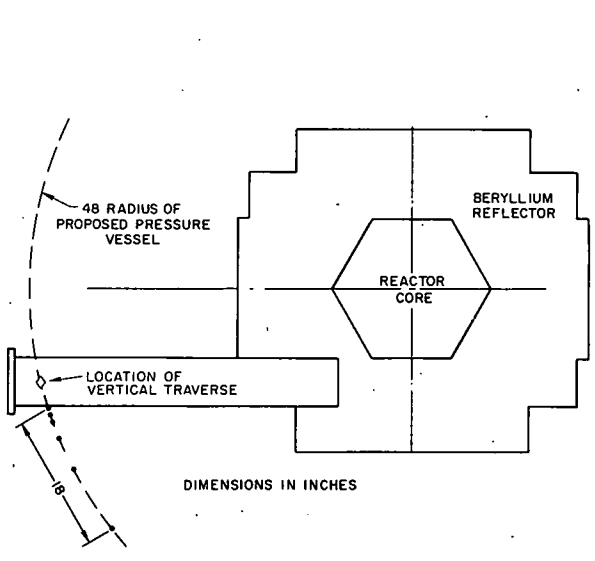

112-8372 Rev. 1

Fig. 19. Probe Positions for Measuring Gamma Heating at Location of AARR Pressure-vessel Wall

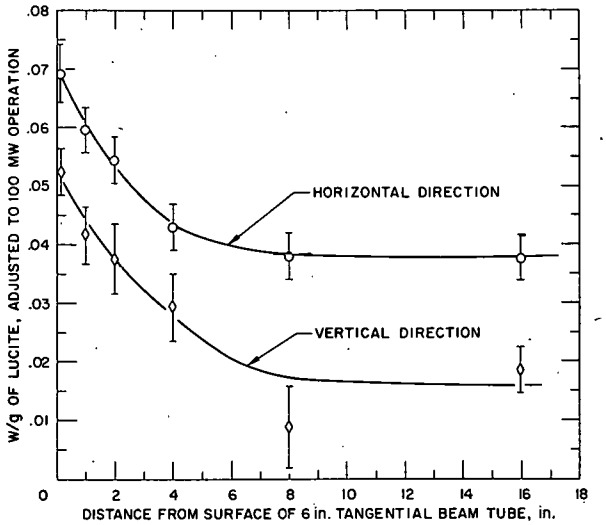

112-8366 Rev. 1

Fig. 20. Gamma-ray Heating at Location of AARR Pressure-vessel Wall. Probe locations are indicated in Fig. 19.

in the horizontal direction, the heating rate falls off by a factor of about two in 6 or 8 in., approaching an asymptotic value of approximately 0.038 W/g. As mentioned before, all power calibrations are subject to an uncertainty of approximately ±15%.

In another experiment, a measurement was made to see whether hot spots would be generated in the wall of the pressure vessel by gamma rays streaming laterally across parallel, or almost parallel, voided beam tubes. Two 6-in.-square tangential beam tubes were placed in the beryllium reflector as shown in Fig. 21, and a vertical TLD traverse was made 48-in. from the center of the reactor, as indicated. For comparison, another such traverse was made simultaneously opposite another face of the reactor, where there were no beam tubes. The results appear in Fig. 22. Although there does appear to be increased heating on the side near the beam tubes, there is no indication of a hot spot due to gamma rays which, travelling upward at an angle, have passed through both beam tubes.

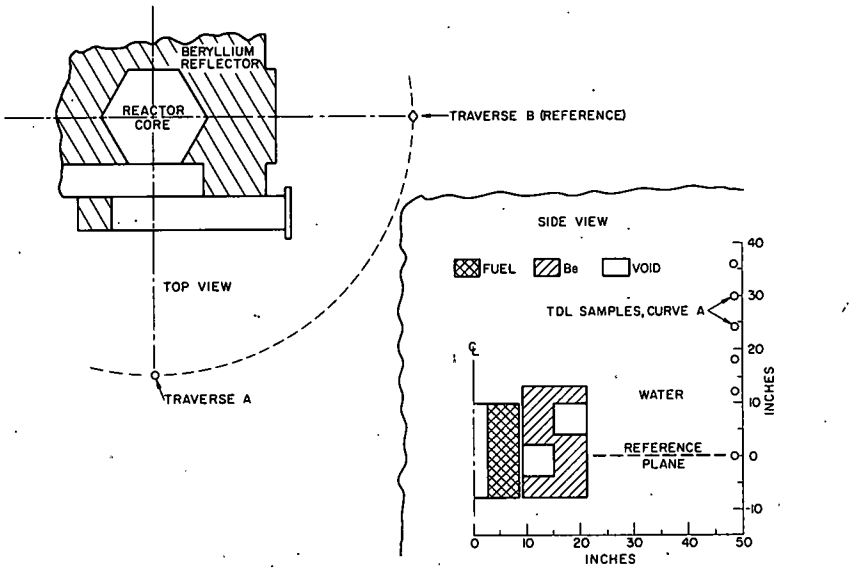

Fig. 21. Arrangement for Investigating Lateral Gamma-ray Streaming across Parallel Voided Beam Tubes

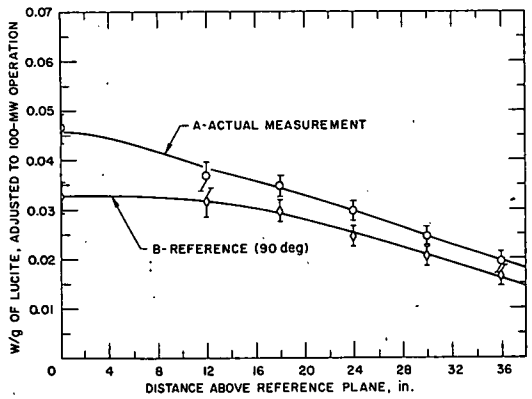

Fig. 22

Gamma-ray Heating at the Location of the AARR Pressure-vessel Wall, with Two Parallel 6-in. Beam Tubes. Probe positions are shown in Fig. 21.

K. Gamma Heating around the Inner Tip of a Tangential Beam Tube

With a 6-in. tangential beam tube located as in Fig. 14, a TLD sample was placed inside it, near the inner tip, at the centerline of each of the four lateral walls. Aluminum capsules were used. The capsules in this case did not contain O-ring seals, but the doses were high enough so that the effect of humidity would be negligible. The results were as follows:

Beam-tube Surface:	Inner	Top	Outer	Bottom
W/g at 100-MW operation:	4.34	2.65	2.38	3.48

The reproducibility of these numbers is approximately ±5%, with the additional uncertainty of ±15% in the power calibration.

L. Comparison of Aluminum, Lucite, and Stainless Steel Capsules

Equation 2.9 states that the ratio of the dose rates in two materials is equal to the ratio of their effective mass energy-absorption coefficients. An experiment was performed to see whether this would be observed. Two capsules each of aluminum, stainless steel, and Lucite were arranged on the bottom of a 6-in. tangential beam tube, as shown in Fig. 23, and the reactor was run so as to give each sample a dose of about 1500 rads.

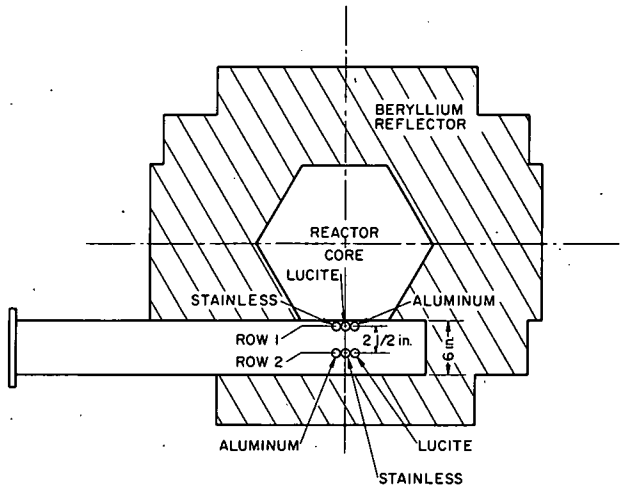

Fig. 23
Probe Locations for Comparing Capsule Materials

The observed results were as follows:

Capsule Material:	Stainless Steel	Lucite	Aluminum
Observed response, arbitrary units			
Row 1:	3.39	2.56	3.04
Row 2:	2.40	1.93	2.01

The data yield these response ratios:

	Row 1	Row 2	Average
Aluminum/Stainless Steel	0.90	0.83	0.87
Aluminum/Lucite	1.19	1.04	1.11

These ratios were calculated on the assumption that there was no lateral gradient of the gamma-ray flux in the voided beam tube, over the 3-in. distance occupied by the capsules. This assumption is consistent with the discussion in Sections V.F and V.G, where it was observed that the asymmetric falloff to the right of the centerline did not occur in a voided beam tube.

The observed ratios should correspond with the ratios of the mass energy-absorption coefficients, and can be compared with Table III, assuming that the coefficient of stainless steel is not very different from that of iron. The two average ratios are roughly in agreement with the corresponding ones in Table III. Unfortunately, the experimental accuracy is not sufficient to permit any firm conclusions to be drawn regarding the low-energy end of the gamma-ray spectrum, although the indications are that the effective energy of the low-energy group, near the core, is less than 0.8 MeV.

M. Comparison with Calculations

Some gamma-ray heating rates to be expected in the critical facility were calculated by McArthy and Shaftman,[11] using the computer program MAC (Multigroup Attenuation Code). It was necessary to assume a simplified geometry for the calculations. The model for the neutron-diffusion portion of the calculations consisted of a spherical core surrounded by 30.5 cm of beryllium and 152 cm of water, while the gamma-ray attenuation was calculated on the basis of infinite-slab geometry. Corrections were applied to convert the results to approximate a finite cylindrical geometry. Since a homogenized core was assumed, the effects of gamma-ray streaming parallel to the fuel plates were not calculated. The power distribution in the core was assumed to be flat, whereas there was in reality power peaking at the outer and inner boundaries--particularly in the ungraded cores. The computed heating rates are plotted in Fig. 24.

The curve marked "measured" in Fig. 24 is synthesized from two of the measurements reported above. The portion outside the beryllium is taken directly from Fig. 18; the inner segment of the experimental curve consists of Traverse 2 from Fig. 9. The inner segment was normalized to match the outer one at the boundary of the beryllium. Traverse 2 was selected because it was least likely to have been affected by gamma-ray streaming and hence should correspond most closely to the conditions of the calculation.

The experimental errors indicated in Fig. 24 represent the estimated reproducibility of the TLD measurements. The experimental curve is also subject to a systematic calibration and spectrum-correction uncertainty of about 20%. An additional uncertainty comes from the fact that the inner part of the experimental curve is from Assembly 3 rather than Assembly 5; however, the shape of the neutron flux in the beryllium was largely independent of core loading, and that might also be expected to apply to the gamma-ray flux.

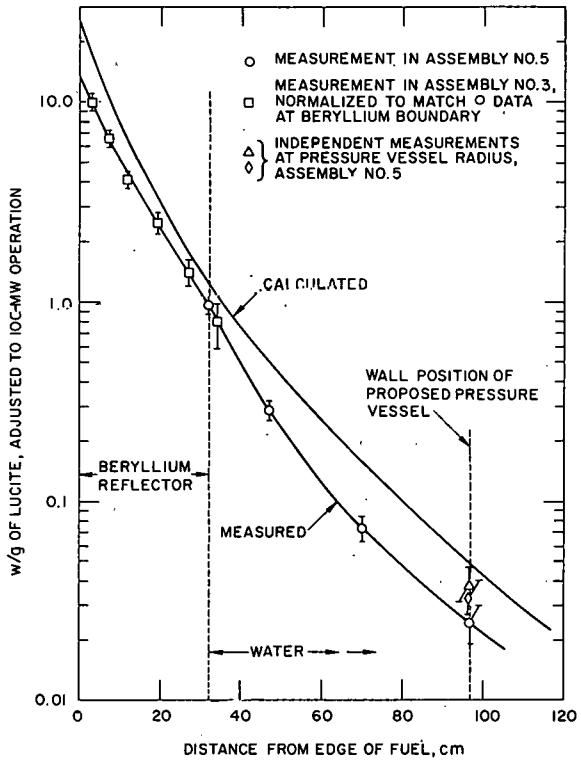

112-9091

Fig. 24. Measured and Calculated Gamma-ray Heating outside the Core of the AARR Critical Assembly

The two extra data points plotted at the position of the wall of the proposed pressure vessel come from Figs. 20 and 22. Although the experimental consistency is not as good as we would like, the scatter is consistent with the experimental calibration uncertainties. Moreover, the three measurements were at different azimuthal locations.

There is some indication of disagreement between calculation and experiment in the beryllium region. In the water outside the beryllium, the discrepancy is worse both in shape and magnitude. However, as this report is going to press, the heating rates calculated by some other codes are becoming available, with indications that the MAC results are too high and otherwise inconsistent.[24] Thus the significance of the calculated curve in Fig. 24 is questionable. Also, the calibration of the experimental curve is based on a single power measurement, and in general there is little in the way of experimental redundancy apart from the three points at the pressure-vessel radius. Time did not permit more experiments to confirm the results.

VI. CONCLUSION

A. Suggested Refinements of Technique

The doses used in this investigation were fairly large, with a lower limit of 5-10 rads. For doses appreciably lower than this the ratio of readout signal to black-body background would need to be reduced

(see Section III.E). Electrical heating, as used in this work, has the disadvantage that the heated region cannot easily be restricted to the area occupied by the powder. Some workers have reported success with small-area heating by radiant energy.[15,17]

If dark current from the photomultiplier tube becomes a problem, this can be alleviated by careful tube selection and by cooling the tube. A chopping technique has also been used to reduce the effect of the dark current.[14]

A spurious thermoluminescence equivalent to a dose as large as 1 rad has been observed in CaF_2:Mn, due to the presence of air.[7] Flooding the powder with dry nitrogen during readout has been suggested for reducing this effect.[13]

If a small, stable light source is available for monitoring the sensitivity of the readout apparatus, comparison with standards irradiated in a calibrated gamma-ray facility would not be needed so often. Small sources excited by a radioactive component are available,* presumably offering more stability than electrical light sources.

B. Summary

Thermoluminescent dosimetry (TLD) with manganese-activated calcium fluoride phosphor has been used successfully to measure gamma-ray heating in the vicinity of the core of a critical facility operating at powers of 20-300 W. The method provides good sensitivity, small probe size, and relative ease of handling and does not require elaborate experimental equipment. The Bragg-Gray principle of cavity ionization has been used in interpreting the results, and appropriate formulas have been presented.

The absolute dose rates were determined by comparing the TLD samples with standards composed of phosphor from the same batch, exposed in a calibrated gamma-ray irradiation facility. Because TLD phosphors have diminished sensitivity to densely ionizing particles, a correction factor is needed to allow for the difference in gamma-ray spectra between the calibration facility and the critical assembly. This factor was determined empirically for one location in the beryllium reflector, in an experiment involving the use of an ion-current chamber (Section V.E). The factor thus determined would also correct for any sensitivity to neutrons, but on the basis of calculations and other experiments it was concluded that any such sensitivity was small.

---

*One supplier of low-intensity, radioactive light sources is American Atomics Corporation, 425 South Plumer Avenue, Tucson, Arizona 85719.

The result of the above experiment indicated that in qualitative agreement with calculations, the gamma spectrum in the beryllium reflector near the core of the reactor had an appreciable low-energy component.

Other experiments indicated that local heating in the beryllium reflector of the AARR critical assembly near the core was a function of the nearby fuel-plate orientation, presumably because of gamma-ray streaming in the water channels.

As one of the major experimental precautions, it was necessary to avoid exposing the phosphor to humidity. We adopted the practice of baking the phosphor for a few hours at about 400°C shortly before use. Also, the capsules in which the powder was irradiated contained O-ring seals.

The reproducibility of the measurements discussed in this report was typically about 5-10%. The absolute measurements were subject to an additional uncertainty of ±15% in the determination of the reactor power, and there was also an uncertainty of approximately ±10% in the spectrum correction factor. Thus the net uncertainty in most of the absolute measurements reported was about ±20% (although occasionally ranging up to ±35%). The principal source of uncertainty in the absolute measurements had to do with the reactor power calibration, rather than the TLD work per se.

ACKNOWLEDGMENTS

We are grateful to H. Frank Reed for the original suggestion that TLD might be applied to the gamma-heating problem. Jacob Kastner gave invaluable advice and information regarding the technique of TLD, and permitted us to use his readout equipment in the initial stages of this work. We are also indebted to Frank S. Williamson for informative discussions, and to him and to Joseph E. Trier for active assistance in using the calibrated Co^{60} irradiation facility. Much help in selecting useful experiments came from David H. Shaftman, Project Physicist for the AARR program. William R. Robinson collaborated in setting up some of the reactor irradiations. The reactor runs were performed with the willing cooperation of the AARR operating crew, under the supervision of Karl E. Plumlee.

REFERENCES

1. F. H. Attix, *Present Status of Dosimetry by Radiophotoluminescence and Thermoluminescence Methods*, Naval Research Laboratory, Report 6145, (Sept. 18, 1964).

2. Z. Spurný, *Thermoluminescent Dosimetry*, At. Energy Rev. *3*, No. 2, 61-115 (1965).

3. L. H. Gray, *An Ionization Method for the Absolute Measurement of γ-Ray Energy*, Proc. Roy. Soc. (London), *A-156*, 578-596 (1936).

4. L. H. Gray, *The Ionization Method of Measuring Neutron Energy*, Proc. Camb. Phil. Soc. *40*, 72-102 (1944).

5. Otto Glasser and John Victoreen, *The Thimble Ionization Chamber*, Radiology *29*, 341-345 (1937).

6. U. Fano, *Note on the Bragg-Gray Cavity Principle for Measuring Energy Dissipation*, Radiation Res. *1*, 237-240 (1954).

7. L. V. Spencer and F. H. Attix, *A Theory of Cavity Ionization*, Radiation Research *3*, No. 3, 239-254 (1955).

8. *Physical Aspects of Irradiation*, Handbook 85, National Bureau of Standards (1964).

9. *Reactor Physics Constants*, ANL-5800, Second Edition (July 1963), p. 654.

10. C. L. Wingate, E. Tochilin, and N. Goldstein, *Response of LiF to Neutrons and Charged Particles*, Naval Radiological Defense Laboratory, USNRDL-TR-909 (Sept. 28, 1965).

11. A. E. McArthy and D. H. Shaftman, Argonne National Laboratory (private communication).

12. Charles Weyl and S. Reid Warren, Jr., *Radiologic Physics*, Charles C. Thomas, Springfield, Illinois (1951), 2nd Edition.

13. Jacob Kastner, Ramesh Hukkoo, and B. G. Oltman, "Lithium Fluoride Thermoluminescent Dosimetry for Beta Rays," *Luminescence Dosimetry*, pp. 482-489, AEC Symposium Series No. 8, Frank H. Attix, (Ed.) (1965).

14. J. Lippert and V. Mejdahl, *Thermoluminescence Read-Out Instrument for Measurement of Small Doses*, Risø Report No. 101 (May 1965).

15. M. Frank and L. Herforth, *Thermoluminescence Dosimetry with $CaF_2(Mn)$*, UCRL-TRANS-1208(L), Translated from Kernenergie *5*, 173-176 (1962).

16. J. R. Cameron, D. Zimmerman, G. Kenney, B. Buch, R. Bland, and R. Grant, *Thermoluminescent Dosimetry Utilizing LiF*, Health Physics *10*, 25-29 (1964).

17. John Cameron, University of Wisconsin, *via* F. S. Williamson, Argonne National Laboratory (private communication).

18. Robert J. Ginther and Russell D. Kirk, *The Thermoluminescence of CaF_2:Mn*, J. Electrochem. Soc. *104*, 365 (1957).

19. R. C. Palmer, E. F. Blase, and V. Poirier, *A Coprecipitation Technique for the Preparation of Thermoluminescent, Manganese-Activated Calcium Fluoride (CaF_2:Mn) for Use in Radiation Dosimetry*, Intern. J. Appl. Radiation and Isotopes *16*, 737-745 (1965).

20. B. G. Oltman, J. Kastner, P. Tedeschi, and J. N. Beggs, *The Effects of Fast Neutron Exposure on Li^7F Thermoluminescence Response to Gamma Rays*, Health Physics *13*, No. 8, 918-919 (1967).

21. D. H. Shaftman and R. P. Savio, Argonne National Laboratory (private communication).

22. D. H. Shaftman and R. P. Savio, *The Argonne Advanced Research Reactor (AARR)*, AEC-ENEA Seminar on Intense Neutron Sources (SINS), Santa Fe, New Mexico, Sept. 19-23, 1966, CONF-660925, pp. 215-259.

23. K. E. Plumlee *et. al.*, "Argonne Advanced Research Reactor Critical Experiments Preface," *Reactor Physics Division Annual Report, July 1, 1965 to June 30, 1966*, ANL-7210 (Dec 1966), pp. 47 and 48.

24. D. H. Shaftman, Argonne National Laboratory (private communication).